Title:	**BRB and FVD Alternatives to Conventional Steel Brace Outriggers**
Authors:	John Viise, Associate Principal, Halvorson and Partners Patrick Ragan, Project Engineer, Halvorson and Partners Jim Swanson, Principal, Halvorson and Partners
Subject:	Structural Engineering
Keywords:	Damping Outriggers Steel Structure
Publication Date:	2014
Original Publication:	CTBUH 2014 Shanghai Conference Proceedings
Paper Type:	1. Book chapter/Part chapter 2. Journal paper 3. **Conference proceeding** 4. Unpublished conference paper 5. Magazine article 6. Unpublished

BRB and FVD Alternatives to Conventional Steel Brace Outriggers

传统外伸臂支撑的替代方案: BRB和FVD

John Viise

Patrick Ragan

Jim Swanson

John Viise, Patrick Ragan & Jim Swanson

Halvorson and Partners (H+P)
600 West Chicago Avenue, Suite 650
Chicago, Illinois
60654 USA

tel (电话): +1 312.981.3330, +1 312 981 2094, +1 312 274 2407
fax (传真): +1 312 274 2401
email (电子邮箱): jviise@hpse.com; pragan@hpse.com; jswanson@hpse.com
hpse.com

John Viise has been providing structural services for high-rise and special-use structures throughout the world for the past 20+ years. . John is also a voting member of the ASCE 41 Standards committee which deals with the development of performance-based design provisions utilized internationally for seismic design.

John Viise在过去20多年里为世界各地的高层结构和特殊用途结构提供结构设计服务。John也是ASCE 41标准委员会中有表决权的会员，ASCE 41标准委员会负责制定地震设计国际通用的性能化设计规定。

Patrick Ragan leads H+P's work on nonlinear analysis and performance-based design. He has developed analytical models for numerous high-rise projects in China and elsewhere. He led the nonlinear geometric form-finding analyses for two shell structures in China, the UAE Pavilion for the 2010 Shanghai Expo, and the Kempinski Residence Roofs in Yinchuan.

Patrick Ragan负责领导H+P的非线性分析和性能化设计工作，他为中国和其他国家的众多高层建筑项目开发了分析模型，其中包括天津万通中心、武汉琴台国际中心、北京三星人寿保险总部、深圳汉京中心、阿布达比中央市场再开发项目以及河内Vietin Bank银行业务中心。他负责了2010年上海世博会阿联酋馆及银川凯宾斯基公寓屋面的壳体结构非线性几何找形分析工作。

James Swanson is a Principal with Halvorson and Partners and a 30-year industry-leading structural engineer. Jim's professional career features extensive experience in a variety of state-of-the-art developments of high-rise, long-span and transportation structures.

James Swanson是H+P的副总裁，也是业界顶级结构工程师之一，30多年来一直走在行业的前列。他有丰富的项目经验，曾参与各类先进的高层结构、大跨度结构和交通结构项目。

Abstract

Tall buildings are often stiffened by providing large steel outrigger braces to link a central core to the perimeter columns. As an alternative to this approach, this study considers two other member types for use at the outrigger locations: a buckling restrained brace (BRB), and a fluid viscous damper (FVD). Although these alternate approaches are less stiff, they provide superior energy dissipation under dynamic loading while avoiding the large localized forces associated with conventional outriggers. Previous outrigger applications of BRBs and FVDs are reviewed, and the fundamental behavior of damping elements is contrasted to that of stiffness elements. The performance of a 260-meter office building using conventional steel brace outriggers is compared to the performance of the BRB and FVD alternate structures for a range of seismic loading, frequent to rare, based on the seismic hazard in Beijing. Using an approximate response spectrum-based method and results from nonlinear response history analysis, the advantages of the alternate schemes are highlighted. Emphasis is placed on the application of the alternative approaches from a designer's perspective.

Keywords: Outriggers, BRB, FVD, Damping

摘要

高层建筑通常用大型外伸臂钢支撑连接中央核心筒和外围框架柱进行加固。本项研究考虑在外伸臂位置使用另外两种构件: 屈曲约束支撑 (BRB又名UBB) 和液体粘滞阻尼器 (FVD) 代替钢支撑方案。虽然替代方案的刚度不如钢支撑，但是替代方案在动态荷载条件下具有优越的能量耗散性能，同时能避免传统外伸臂结构的局部应力集中现象。本文回顾了BRB和FVD作为外伸臂的早期应用，比较了阻尼构件与刚性构件的基本性能。以北京的地震灾害为基础，比较了260米办公楼采用传统外伸臂钢支撑结构与BRB和FVD替代结构在不同地震作用下的性能表现。用近似反应谱方法和非线性时程分析的结果介绍了替代方案的优势。本文着重从设计师的角度出发介绍了替代方案的应用。

关键词: 外伸臂、屈曲约束支撑 (BRB) 、液体粘滞阻尼器 (FVD) 、阻尼

Structural Systems Featuring Outriggers

Outrigger systems are prevalent in the structural design of tall buildings because they efficiently increase structural stiffness by linking building cores with perimeter columns to resist overturning forces. In addition, outriggers relieve overturning stresses in a building's core by sharing the loads with the perimeter columns, all while avoiding the architectural disruption of having continuous fin walls or bracing linking the core to the perimeter columns throughout the height of the building.

Concentrating the transfer of overturning forces to just a few discrete structural elements, however, results in very large localized forces at the linking locations. Often the resulting 'panel zone' shear forces are greater than the base shear for the entire building, and thicker concrete walls and embedded structural steel braces are required to resist these forces (see Figure 1). As a result, material costs, construction complexity and schedule time for an outrigger level are significantly greater than for a typical tower level.

外伸臂结构体系

外伸臂结构体系通过连接建筑核心筒和周边框架柱形成抗倾覆力，能有效提高结构刚度，在高层建筑结构设计中的使用非常普遍。外伸臂结构与周边框架柱一起承担荷载，降低核心筒的倾覆力，因而不需要在建筑物全高设置连续的翼缘墙或连接核心筒和周边框架柱的支撑，从而避免了打断建筑的连续性。

倾覆力集中传递到少数几个结构构件会在连接位置产生极大的局部应力。由此产生的'板域'的剪力通常大于整个结构的基底剪力，从而需要设置较厚的混凝土墙和预置钢结构支撑来抵抗剪力 (参见图1) 。因此，外伸臂层的材料费、施工复杂度和工期远远超过标准楼层。

除了费用外，人们普遍认为设置大型外伸臂钢支撑是高层建筑的有效加固措施。但是，增加刚度并非控制建筑运动的唯一控制方法。

Despite these costs, it is generally agreed that providing large steel outrigger braces is an efficient strategy for stiffening a tall building. Providing added stiffness, however, is not the only way to control building movements.

Damping as an Alternative to Stiffness

Increasing damping, either in the form of pure viscous damping or hysteretic yielding, can be more effective than increasing stiffness for limiting movements and improving a building's performance under dynamic lateral loads. A structural solution which controls movements without increasing stiffness is especially attractive for resisting seismic loads, since structures with less stiffness (and longer periods) experience lower seismic forces.

For the design of a new 260-meter, 59-story composite tower in Beijing, Halvorson and Partners (H+P) considered two alternative member types – a buckling restrained brace (BRB) and a fluid viscous damper (FVD) – for use in place of a conventional steel brace at the outrigger locations. In the study that follows, three versions of the tower are compared under seismic loading. The first uses large conventional steel braces (axial yield force Py = 67,000 kN), the second uses smaller BRBs (Py = 5000 kN), and the third uses FVDs (rated force of 5000 kN). Comparisons are made between the three schemes for overturning moment, drift, energy dissipation, and estimated damage to the remainder of the structural system. The goal is to compare the performance of the alternate systems – which have increased damping but reduced stiffness – with the performance of the conventional steel outrigger base scheme.

BRB Outriggers

A BRB is designed to avoid buckling and strength loss under increasing compressive force, instead yielding in compression similarly to how a brace yields in tension. As a result, the hysteresis loops of a BRB are not pinched in the same way as the post-buckling hysteresis loops of a conventional steel brace. The larger areas encompassed by the BRB loops correspond to significantly larger amounts of energy dissipation under cyclic seismic loading.

In theory a BRB could be equally stiff as a conventional outrigger, and merely improve upon the conventional brace behavior by not buckling in the inelastic region. However, practical limitations in manufacturing and testing dictate that BRBs cannot be arbitrarily large. For the purposes of this study a yield force of 5000 kN has been assumed, which is roughly equal to the yield capacities of the BRB outriggers designed and used on One Rincon Hill project in San Francisco (Klemencic, Hooper & Johansson 2006).

FVD Outriggers

A viscous damping element behaves fundamentally differently from a conventional structural element. A damping element resists velocity (v) rather than displacement (u), with the magnitude of the resisting force (F) described by the following relationship:

$$F = cv^a$$

where c is the damping coefficient, and a is the damping exponent.

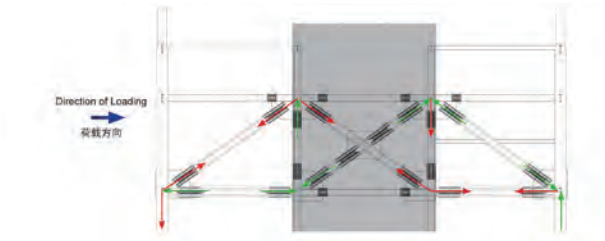

Figure 1. Steel outrigger braces linking concrete core to perimeter columns. Large 'panel-zone' shear forces are resisted by steel brace elements embedded within the concrete core walls. (Source: Halvorson and Partners)
图1: 连接核心筒和周边框架柱的外伸臂钢支撑。混凝土核心墙的预埋钢支撑构件抵抗大量的水平**向剪力 (资料来源: 美国H+P建筑结构事务所)**

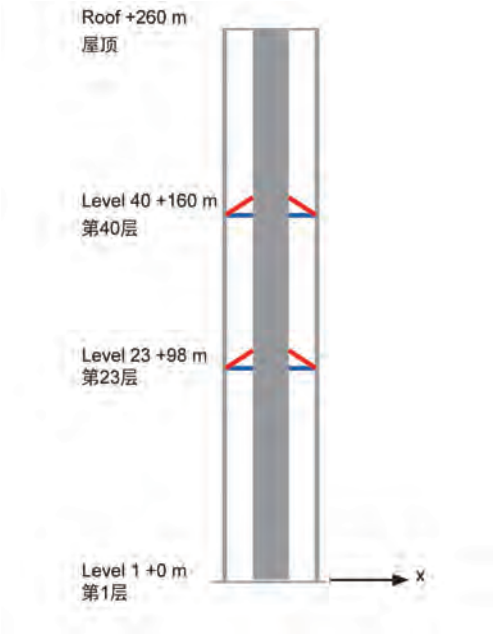

Figure 2. System diagram. Concrete core walls are linked to perimeter columns at two double-story height (8.4 m tall) mechanical levels. Outrigger elements (red) are typically large steel braces; BRB and FVD alternatives are considered in this study. (Source: Halvorson and Partners)
图2: 体系示意图。在两层高 (8.4米高) 设备层，混凝土核心筒与外框架柱连接。外伸臂构件 (红色) 一般是大型钢支撑; 本项考虑了两种代替方案 - BRB和FVD (资料来源: 美国H+P建筑结构事务所)

阻尼代替刚度

与提高刚度相比，提高纯粘滞阻尼或滞回屈服耗能更有效地限制建筑运动和提高建筑物在横向动力荷载下的性能。结构的刚度越小 (周期越长)，受到的地震作用就越小，因此，既能控制运动，又不增加刚度的结构方案是特别优异的抗震方案。

关于北京260米59层新建混合结构大楼的设计，美国H+P建筑结构事务所考虑在外伸臂位置采用两种替代构件——屈曲约束支撑 (BRB) 和液体粘滞阻尼器 (FVD) ——代替传统的钢支撑。在后续研究中，比较了大楼三个设计方案在地震作用下的性能。第一个方案使用传统的大型钢支撑 (轴向屈服力Py = 67,000 kN)，第二个方案使用较小的BRB ((Py = 5000 kN)，第三个方案使用FVD (额定力为5000 kN)。对三个方案的倾覆力矩、侧移、能量耗散以及结构体系其余构件的估计破坏进行了比较。目标是比较替代体系的性能 (替代体系增加了阻尼，降低了刚度) 与传统钢伸臂基础方案的性能。

Conceptual Comparison Between Stiffness Outriggers and Damping Outriggers

The distinction between resisting displacement and resisting velocity may seem academic, since velocity and displacement are related by $v = du/dt$, so if an element reduces displacement then it has also reduced velocity (and vice versa). However, displacement and velocity are out of phase with each other, and this is a critical point which explains the advantage of a damping element for resisting dynamic loads.

This may be illustrated by considering a simple, physical example in which a building is displaced into its primary mode shape, then is released into free vibration from this initial displacement (see Figure 4). Two cases are considered – one where the outrigger is a conventional stiffness element, and another where the outrigger is a damping element with $\alpha = 0.3$.

Referring to Figure 4c (damper outrigger) and Figure 4d (conventional stiffness outrigger), note the difference in the direction of the outrigger forces as the building sways from the initial peak at time step 0 to the opposite peak at time step 4. Between peaks the damper is always opposing motion towards the next peak. Kinetic energy of the building's motion is absorbed by the damper (converted into heat), reducing the building's velocity and displacement. On the other hand, between steps 0 and 2 the forces in the conventional outrigger are actually inducing motion towards the peak displacement at step 4, as strain energy is converted to kinetic energy. The conventional outrigger does not begin opposing the building's increasing displacement until step 2 (a half cycle later than the damper). Also note that an elastic stiffness element does not dissipate energy; energy is just cycled between strain energy and kinetic energy.

This is a physical description of why a damping element has an advantage is resisting dynamic loads – a damper is always resisting motion towards the next peak displacement. Compared to the stiffness outrigger, the damper has a significant "head start" in opposing the building movement. This allows the damper to be more efficient, with the ability to effectively resist building movements with lower forces than a conventional member.

FVDs in Buildings

Fluid viscous dampers have been used in many completed projects, including the 225-meter Torre Mayor in Mexico City (Taylor 2003) and the retrofit of 28 State Street in Boston (McNamara, Huang & Wan 2000). In both of these cases, a number of dampers are distributed uniformly throughout the height of the building to provide additional damping relatively equally for all the building's modes of vibration. The advantage of arranging dampers this way is that it allows a building to be analyzed using simplified methods such as the modified response spectrum procedure in Chapter 18 of ASCE 7-10.

An alternative approach is to use fewer dampers, placing them only at selected locations where they are most effective. For a high-rise building, the most obvious choice is to put the dampers at outrigger locations. At these locations, large relative vertical displacements between the core and perimeter frame induce significant forces and strokes in the dampers, maximizing energy dissipation per damper. This is the approach advocated by Smith and Willford (2007) and used in the design of London's Pinnacle Tower and 250 W 55th St in New York.

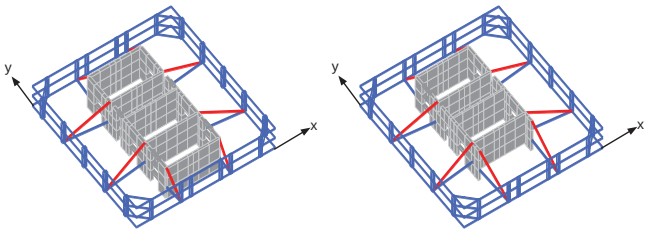

Figure 3. Outrigger level isometrics, levels 23-25 (left) and levels 40-42 (right) (Source: Halvorson and Partners)
图3: 外伸臂楼层的等轴视图。23-25层 (左) 和40-42层 (右) (资料来源: 美国H+P建筑结构事务所)

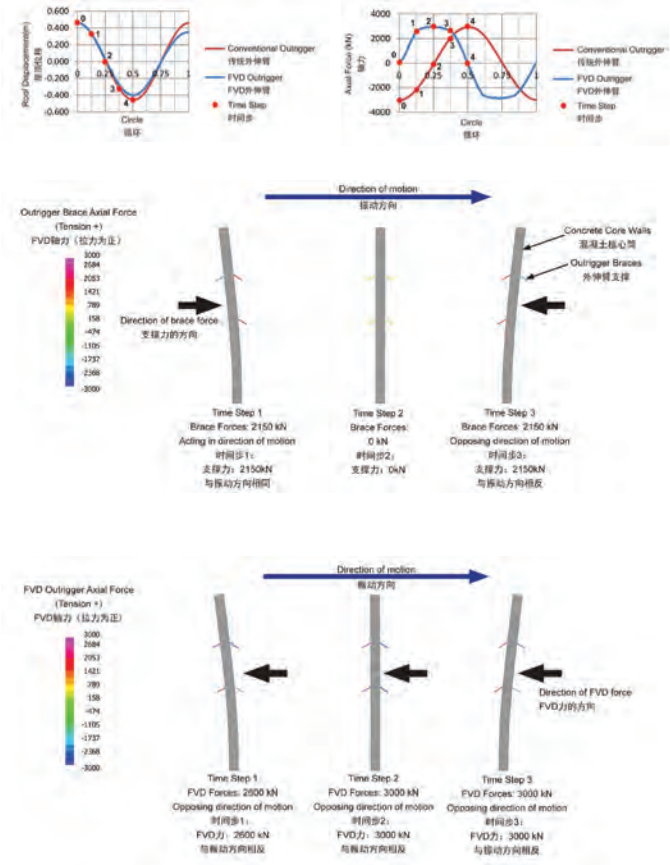

Figure 4. Comparison of free vibration response, conventional outrigger and FVD outrigger. FVD is 90 degrees out-of-phase relative to the conventional outrigger and always opposes the building's direction of motion. (Source: Halvorson and Partners)
图4: 传统外伸臂和FVD外伸臂自由振动响应比较。FVD与传统的外伸臂有90度的相位差并总与结构振动方向相反 (资料来源: 美国H+P建筑结构事务所)

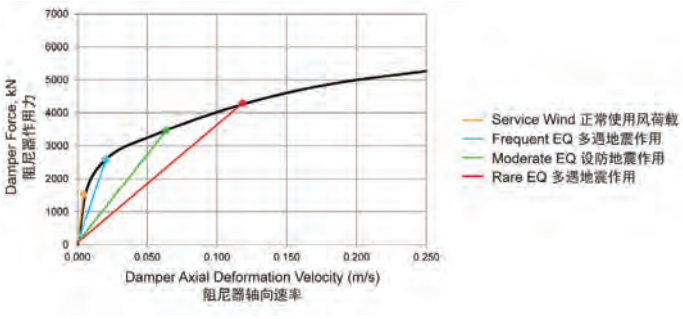

Figure 5. Damper force-velocity relationship, $F = 8100v^{0.3}$, units in kN and m/s. Varying slopes of secant lines indicate varying levels of damping under various load cases. (Source: Halvorson and Partners)
图5: 阻尼器力与速度关系图，$F = 8100\,v^{0.3}$，单位kN和m/s. 不同的割线斜率表示各种荷载工况下的不同阻尼。(资料来源: 美国H+P建筑结构事务所)

Selection of Damper Coefficient and Exponent

The coefficient c in equation 1 is proportional to the damper force, and the damper force is the greatest driver of the damper's cost, so c should be selected carefully. For a system of uniformly distributed dampers, increasing c for each individual damper will increase the global damping (typically expressed as a percent of critical damping) proportionally. For a damper outrigger system, the relationship is more complicated, since extremely high resistance in the dampers (in the limit, a rigid damper) would simply cause the system to deform around it, which in turn would limit the effectiveness of the damper. Therefore, a prudent approach is to consider a series of different values of c, and determine the optimal choice based on the building's performance as well as the damper's cost.

The damper exponent is also selected by the designer, typically with $0.3 < a < 1.0$. Using a sub-linear exponent ($a<1$) is often desirable, because it allows larger amounts of damping to take place under service conditions (which the building experiences most often, and is most relevant to occupant comfort) while protecting the damper from being overloaded and failing under extreme conditions. For this study, the values of c and a were chosen to be 8100 and 0.3, respectively, with units in kN and m/s. Figure 5 illustrates varying damping resistance under various wind and earthquake levels.

Estimation of Global Damping

It is useful for benchmarking purposes to estimate global damping ratios for structures with supplemental damping. There are two main issues that complicate this computational effort. First, a sub-linear damper ($a< 1$) will have different damping ratios depending on the amplitude of displacement. For this reason, unique global damping ratios must be calculated for each unique type of loading (e.g. service wind, frequent earthquake, rare earthquake, etc.). Secondly, each mode will in general have a different level of global damping, and a system with only a few isolated damping elements may be expected to have higher variability in damping between modes than a system with a more uniform distribution of dampers.

Nevertheless, it is helpful to quantify an approximate 'overall' damping ratio for a given load case, as this will facilitate preliminary estimates of building performance, as described in a later section. A simple

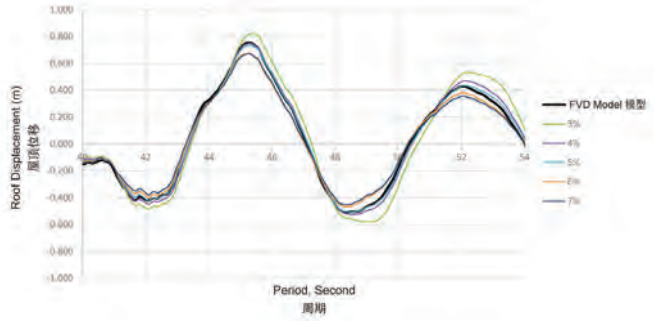

Figure 6. Estimation of global damping, selected segment of sample moderate earthquake response history. Results from an analysis model which includes the FVDs and 2% inherent damping are compared to models which omit the FVDs and have varying levels of inherent damping. For moderate earthquake the FVD model results closely match the results for 5% damping, implying a 3% contribution from the FVDs. (Source: Halvorson and Partners)

图6: 示例为设防地震作用响应时程分析的部分时段的总体阻尼的估算。对包括液体粘滞阻尼和2%非结构阻尼的分析模型和不包括液体粘滞阻尼但具有不同水平非结构阻尼的模型的结果进行了比较。对于设防地震作用，FVD模型非常接近5%阻尼的结果，这暗示了FVD提供了3%的阻尼。(资料来源: 美国H+P建筑结构事务所)

BRB外伸臂

BRB的原理是防止在压力作用下发生屈曲和强度损失，而是在压力作用下屈服，与支撑在拉力作用下屈服相类似。因此，BRB的滞回曲线不像传统钢支撑的滞回曲线那样收缩。BRB滞回曲线包围的面积增大，与往复地震作用下能量耗散大量增加相对应。

从理论上看，BRB的刚度可与传统外伸臂相同，只是通过在非弹性区域防止屈曲来改善传统支撑的性能。但是，由于实际生产和测试条件的限制，不可能生产任意尺寸的BRB。本次研究假设BRB的屈服力是5000 kN，与旧金山One Rincon Hill项目 (Klemencic，Hooper & Johansson 2006) 设计、使用的BRB伸臂屈服承载力基本相同。

FVD外伸臂

粘滞阻尼构件的特性完全不同于传统的结构构件。阻尼构件抵制的是速度 (v)，而不是位移 (u)，其阻力 (F) 用下式计算:

$F = cv^{\alpha}$

式中，c是阻尼系数，a是阻尼指数。

刚性外伸臂和阻尼外伸臂的概念比较

由于速度和位移具有如下关系: $v = du/dt$，因此抵抗位移与抵抗速度具有理论差别，构件在降低位移时也会降低速度 (反之亦然)。但是，位移和速度相位不同，这是一个关键点，解释了阻尼构件更能抵抗动力荷载的原因。

下面举一个简单的实例进行说明，实例中先使建筑物位移至主振型，然后使建筑物从初始位移状态开始自由振动 (参见图4)。考虑两种情况，第一，外伸臂采用传统刚性构件; 第二，外伸臂采用阻尼构件，$a = 0.3$。

参见图4c (阻尼器外伸臂) 和图4d (传统刚性外伸臂)，注意观察建筑物从时间步0的初始峰值移到时间步4的对应峰值期间的外伸臂受力方向的变化。在两个峰值之间，阻尼器始终阻止建筑物移向另一个峰值。阻尼器吸收建筑物的运动动能 (转化为热能)，降低建筑物的运动速度和位移。另一方面，在时间步0和时间步2之间，传统外伸臂力实际上通过把应变能转化为动能促使建筑移向时间步4的峰值位移。传统外伸臂直到时间步2才开始阻止建筑物位移的增加 (比阻尼器晚半个周期)。另外还可以看出，弹性刚性构件没有耗能作用; 能量只是在应变能和动能之间循环。

这个例子说明阻尼构件具有更好的抵抗动力荷载性能——阻尼器总是阻止建筑物移向下一个峰值位移。与刚性外伸臂相比，阻尼器在阻止建筑运动方向具有很大的"先机"。因此，阻尼器能以小于传统构件的力有效地阻止建筑运动，是一种更高效的构件。

建筑中的FVD

FVD已成功运用在多个竣工项目中，包括墨西哥225米的市长大楼 (Taylor 2003年) 及波士顿28 State Street的翻新项目 (McNamara, Huang & Wan 2000年)。在这两个项目中，整个建筑高度均匀地分布着许多阻尼器，为建筑所有的振型提供相对等值的附加阻尼。这种阻尼器布局的优势是可以采用简化方法分析建筑，如美国土木工程师协会ASCE 7-10第18章的改进反应谱法。

还有另外一种方案可以采用较少的阻尼器，仅将其设置在阻尼器最有效的特定位置。对于高层建筑，最显而易见的位置就是外伸

method for this is as follows: First, run a response history analysis of the full model with damping elements. Next, run a series of time history analyses of a model without the damping elements, but with varying amounts of non-structural damping. By determining which of these analyses most closely match the full model analysis, the effective damping ratio may be estimated (see Figure 6). Using this approach, the effective global damping ratios (in addition to inherent damping) provided by the outrigger dampers were estimated to be 5% at the frequent earthquake level, 3% at the moderate earthquake level, and 2% at the rare earthquake level.

Influence of Supplemental Damping on Wind Loads

Equivalent static wind loads for the scheme with damper outriggers were calculated by the Boundary Layer Wind Tunnel Laboratory following wind tunnel testing. Two sets of values were reported – with and without consideration of the supplemental damping provided by the damping outriggers. Based on a free vibration analysis of the system using initial displacements corresponding to predicted dynamic portion of the wind displacement (approximately 30 mm at roof level), the damper outriggers were estimated to contribute 4.5% supplemental damping at 50-year wind loading levels. This is slightly less than was estimated above for frequent earthquake, in part because friction forces slightly reduce the forces in the dampers under the extremely small displacements which would be induced under service wind conditions.

The inclusion of the supplemental damping, in combination with the assumed 1.5% non-structural damping, reduced the overturning moment by 39% under 50-year equivalent static wind forces in the x-direction. In addition, the 10-year maximum x-direction accelerations at the highest occupied floor were reduced by 47%. Although the caveats described in the previous section Estimation of Global Damping are applicable, and a more accurate technique would be to apply time-varying wind loads to the model in a response history analysis, these results clearly demonstrate that substantial improvements to the structural performance are made possible by the dampers.

Seismic Criteria

Table 1 lists the response spectrum parameters a_{max} and T_g for a site in Beijing with Type II soil classification according to the governing Chinese Code, GB50009-2012. Spectral design parameters are shown for the frequent, moderate, and rare earthquake levels, along with corresponding IBC parameters SMS and SM1. For the purposes of this study, the standard form of the response spectrum as defined by IBC Code is used (see Figure 7).

Based on the rare earthquake (MCE) response spectrum, seven pairs of ground acceleration time history records are selected and spectral matching techniques are applied to ensure an appropriate match for each record. For the moderate and frequent levels, the rare time histories are scaled according to the appropriate amax for each level.

Spectral Estimates for Comparative Force and Displacement Demand

Ultimately the force and displacement demand for each of the three schemes are determined from nonlinear response history analysis, but preliminary estimates for these quantities can be obtained simply from the periods and damping ratios for each structure, in conjunction with

臂位置。在这些位置，核心筒及周围框架之间相对较大竖向位移会使阻尼器产生巨大阻力及轴向位移，最大化每个阻尼器的能量耗散。这是由Smith和Willford (2007年) 提出的方法，且在伦敦的尖峰塔及纽约西第五十五大街250号项目中得到了运用。

阻尼器系数及指数的选择

等式1中的系数c与阻尼力成正比，阻尼力是决定阻尼器成本的最大因素，因而系数c应仔细选定。对于阻尼器均匀分布的系统，提高每一个阻尼器的c值将成比例地增加整体阻尼 (主要以临界阻尼的比例来表示) 。对于外伸臂阻尼器系统，关系则更加复杂，因为阻尼器极高的阻力 (在极端情况下，刚性阻尼器) 将引起体系的变形，进而限制了阻尼器的有效性。因此，比较谨慎的方法就是考虑一系列不同的c值，在综合考虑额建筑性能及阻尼器成本的基础上决定最优c值。

阻尼器指数也由设计师选定，通常0.3 <a< 1.0。采用次线性指数 (a<1)是比较理想的做法，因为这样大量的阻尼作用将在正常使用状态 (建筑最常见的条件，也是与住户舒适度最相关的因素) 下产生，这样可以保护阻尼器在极限状态下避免出现超载及故障。在这项研究中，c值及a值分别取8100 kN 与0.3。图5说明了不同风荷载和地震作用下的不同阻尼力。

总体阻尼的估算

为了基准比较的目的，评估有附加阻尼的结构的总体阻尼比是十分有益的。两个主要原因使计算工程量变得复杂。首先，次线性阻尼器(a< 1)的阻尼比由于位移振幅的不同而不同。因此，必须计

	中国规范 Chinese Code		IBC	
地震作用水平 Earthquake Level	α_{max}	T_g	S_{MS}	S_{M1}
	(g)	(s)	(g)	(g)
多遇 Frequent	0.160	0.40	0.160	0.064
设防 Moderate	0.450	0.40	0.450	0.180
罕遇 Rare (MCE)	0.900	0.40	0.900	0.360

Table 1. Seismic Parameters (Source: Halvorson Partners)
表1: 地震参数 (资源来源: 美国H+P建筑结构事务所)

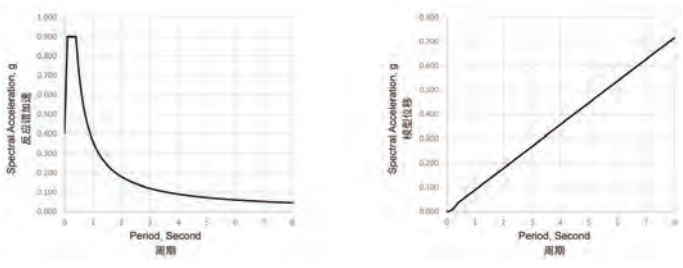

Figure 7. Rare EQ pseudo-acceleration response spectrum (left) and corresponding displacement response spectrum (right), based on $S_{MS} = \alpha$max = 0.90 g, TS =Tg = 0.40 s and 5% damping. (Source: Halvorson and Partners)
图7: 基于$S_{MS} = \alpha$max = 0.90 g, TS =Tg = 0.40 s 和 5%阻尼，罕遇地震的伪加速度反应谱 (左) 和相应的位移反应谱 (右) (资料来源: 美国H+P建筑结构事务所)

the response spectrum. Table 2 lists the periods for the primary mode (x-direction translation) for each structure, as well as the estimated damping ratios for each level of earthquake. Based on these damping ratios, table 18.6-1 in ASCE 7-10 is used to estimate a damping reduction factor B which quantifies how much seismic forces and displacement are reduced for different levels of damping.

The next step is to record the mode 1 spectral accelerations A for each model based on the period and corresponding ordinate of the response spectrum, allowing a quick comparison between the force demands for each structure. In addition, it is useful to consider the spectral displacement form of the response spectrum (obtained using the relation $D = A\,(T_n / 2\pi)^2$) to estimate displacement demands for each structure.

Once A and A are obtained from the respective response spectra, they are divided by the appropriate B values to account for the varying amounts of damping, and comparisons between each structure can be made. As the results for spectral acceleration show, seismic forces are predicted to be 5-10% less for the BRB scheme than for the conventional scheme, and 25-40% less for the damper scheme. For displacements, the damper scheme is predicted to have the

		外伸臂类型 Outrigger Type		
		传统钢支撑 Conventional	屈曲约束支撑 BRB	液体粘滞阻尼器 FVD
抗拉承载力 Tension Capacity, kN	P_t	67,000	5,000	5,000
抗压承载力 Compression Capacity, kN	P_c	32,000	5,000	5,000
基本周期 Fundamental Period	T_x	5.53 s	5.87 s	6.58 s
估算阻尼比 Estimated Damping Ratios	z_{rare}	0.020	0.025	0.040
	z_{mod}	0.020	0.020	0.050
	z_{freq}	0.020	0.020	0.070
阻尼系数 Damping Coefficient	B_{rare}	0.80	0.83	0.93
	B_{mod}	0.80	0.80	1.00
	B_{freq}	0.80	0.80	1.08
底部剪力系数 (g) (反应谱加速度)，5%阻尼 Base Shear Coefficient(g) (Spectral Acceleration), 5% Damping	A_{rare}	0.065	0.061	0.055
	A_{mod}	0.033	0.031	0.027
	A_{freq}	0.012	0.011	0.010
反应谱位移，5%阻尼 (m) Spectral Displacement, 5% Damping	D_{rare}	0.49	0.53	0.59
	D_{mod}	0.25	0.26	0.29
	D_{freq}	0.09	0.09	0.10
底部剪力系数 (g) (反应谱加速度)，根据阻尼调整 Base Shear Coefficient (Spectral Acceleration), Adjusted for Damping	A_{rare}	0.081	0.074	0.059
	A_{mod}	0.041	0.038	0.027
	A_{freq}	0.014	0.014	0.009
反应谱位移，根据阻尼调整 (m) Spectral Displacement, Adjusted for Damping	D_{rare}	0.62	0.63	0.63
	D_{mod}	0.31	0.33	0.29
	D_{freq}	0.11	0.12	0.10

Table 2. System Comparison and Spectral Estimates for Force and Displacement Demand (Source: Halvorson Partners)
表2: 体系比较以及力和位移需求的反应谱估计值 (资源来源: 美国H+P建筑结构事务所)

算每种不同的荷载工况 (如风、多遇地震及罕遇地震等) 下的不同总体阻尼比。第二，每个振型通常对应不同水平的总体阻尼，仅含有一些独立阻尼构件的体系比含有均匀分布阻尼器体系的阻尼可变性将会更大。

然而，近似量化某一给定荷载工况的"总体"阻尼比是非常有用的，因为这将有利于后续章节所描述的对建筑性能的初步估算。一个简单的量化方法即: 首先，对含阻尼构件的全模型进行时程分析; 其次，对无阻尼构件但非结构阻尼不同的全模型进行一系列时程分析，通过确定最接近含阻尼构件的全模型的分析，对有效阻尼比率进行估算 (参考图6) 。采用这一方法，外伸臂阻尼器提供的有效总阻尼比 (除固有阻尼) 在多遇地震作用时约为5%，在设防地震作用时为3%，在罕遇地震作用时为2%。

附加阻尼对风荷载的影响

边界层风洞实验室通过风洞试验计算了阻尼器外伸臂方案的等效静风荷载，报告了两组数据，一组考虑阻尼器外伸臂的附加阻尼，另一组不考虑阻尼器外伸臂的附加阻尼。基于系统自由振动分析，采用与预测的风位移动态部分相对应的初始位移 (顶层约为30mm) ，估计阻尼器外伸臂能为50年一遇的风荷载提供4.5%的附加阻尼，略低于前文多遇地震作用的估计值，其中的部分原因为在正常使用风荷载引发的极其微小的位移情况下，摩擦力略微地减少了阻尼力。

附加阻尼与假设的1.5%非结构阻尼相结合，使50年一遇的等效静风荷载作用下的x向的倾覆力矩减少39%。另外，最高入住楼层x向10年一遇的最大加速度减少47%。虽然之前章节所述的"总体阻尼的估算"的方法是适用的，但更准确的方法是对模型施加时变风荷载并进行时程分析，最终结果清楚地表明，阻尼器能极大地改善结构性能。

抗震标准

表1列出了位于北京按中国荷载规范 (GB50009-2012) 属II类场地的反应谱参数amax 和Tg。另外还列出了多遇地震、设防地震和罕遇地震的反应谱参数以及相应的IBC参数SMS和SM1。在本次研究中，反应谱的标准形状以IBC规范的定义为准 (参见图7) 。

根据罕遇地震 (MEC) 反应谱，选择7组地表加速度时程记录，采用反应谱匹配技术确保为每一条记录找到合适的匹配值。对于多遇和设防地震，按其amax相应地调整罕遇地震时程记录。

等效力和位移需求的反应谱估算

最终这3种设计形式的受力和位移需要均由非线性时程分析得到，但是这些量的初步估算可以简单地通过每个结构的周期和阻尼比，结合反应谱获得。表2为各个结构的主振型 (x向平移) 周期以及各级地震的估计阻尼比。以阻尼比为基础，用ASCE 7-10表18.6-1对阻尼衰减因子B进行估算，从而量化对不同阻尼水平对地震力和位移折减。进一步按照周期和相应的反应谱坐标，记录各个模型振型1反应谱加速度A，从而可以快捷地比较各个结构的受力。此外，使用反应谱得到的位移 (用式$D = A\,(T_n / 2\pi)^2$计算) 对估算各个结构的位移需求是十分有用的。

从相应的反应谱获得A和D后，除以相应的B值以考虑不同的阻尼大小的影响，然后可对不同的结构进行比较。如反应谱加速度的结果所示，预计BRB方案的地震力比传统方案小5~15%，阻尼器方案比传统方案小25~40%。对于位移，预计阻尼器方案在多遇和设防地震作用下的位移最小，但传统方案在罕遇地震作用下的位移最小。

lowest movements under frequent and moderate earthquake, but the conventional scheme has the lowest movements under rare earthquake.

Nonlinear Response History Analysis

The force and displacement estimates described in the previous section are quite useful for understanding how the global behavior of the structure is influenced by such simple parameters as the period and damping ratio. But they are also approximate, having considered only a single mode and not directly including the effects of nonlinear behavior. A more thorough approach, of course, is to evaluate structural performance using nonlinear response history analysis.

At each of the three seismic levels, the same seven orthogonal pairs of ground motion time history records have been applied to each of the three models (Conventional Outrigger, BRB Outrigger, and FVD Outrigger) in a series of nonlinear response history analyses. The three models are each built in CSI's Perform 3D software, and are exactly the same except that the outrigger member is different for each model, and the damper model does not include a belt truss. The models consider P-Delta nonlinearity in addition to material nonlinearity in the outriggers, core walls, perimeter columns, perimeter beams, and belt trusses; nonlinear member response is based on parameters from ASCE 41-06. Inherent damping of 2% is assumed in all cases.

响应量 Response Quantity	地震作用水平 EQ Level	外伸臂类型 Outrigger Type		
		传统钢支撑 Conventional	屈曲约束支撑 BRB	液体粘滞阻尼器 FVD
X向底部倾覆力矩，MN-m Base Overturning Moment X	罕遇 Rare	9,219	8,229	7,650
	设防 Moderate	6,770	5,949	5,015
	多遇 Frequent	3,222	3,029	2,054
X向最大层间位移比 Maximum Interstory Drift Ratio X	罕遇 Rare	H/149	H/136	H/125
	设防 Moderate	H/222	H/222	H/228
	多遇 Frequent	H/501	H/468	H/595
外伸臂能量耗散，kN-m Energy Dissipated by Outrigger	罕遇 Rare	0	8,531	37,699
	设防 Moderate	0	1,117	18,140
	多遇 Frequent	0	0	3,653
其它结构构件能量耗散，kN-m Energy Dissipated by Other Structural Elements	罕遇 Rare	159,171	143,270	118,235
	设防 Moderate	29,896	27,647	18,877
	多遇 Frequent	806	929	355

Table 3. Nonlinear Seismic Response History Results (Average of 7 records) (Source: Halvorson and Partners)
表3: 非线性地震时程分析结果 (取7组时程分析结果平均值) (资源来源: 美国H+P建筑结构事务所)

Nonlinear Response History Results

Table 3 summarizes the results from the time history analyses. The four results being considered are the base overturning moment in the x-direction, the maximum inter-story drift in the x-direction, the amount of energy dissipated by the outrigger elements, and the amount of energy dissipated by the remaining elements of the structural system (link beams, core walls, frame beams, and belt truss). This last quantity may be considered a measure of how much damage is taken by these other structural elements.

For each model and earthquake level, the average of the results for the seven time history analyses is reported. The results show similar trends as the approximate results in the previous section, with the longer periods and greater damping of the BRB and FVD schemes leading to lower forces and greater energy dissipation than the conventional scheme. This, in turn, leads to less energy dissipation observed in the other structural elements, which implies reduced structural damage for the BRB and FVD schemes.

Comparing the BRB scheme to the FVD scheme, it is clear that the damper scheme dissipates considerably more energy, particularly for lower seismic demands, as the BRB remains elastic under frequent earthquake and undergoes only modest yielding under moderate earthquake. The hysteresis plots in Figure 8 illustrate the different behaviors between the two elements, as well as the differing magnitudes of energy dissipation for a sample time history. Similarly the plots in Figure 9 show the relative contributions of various element types to the energy dissipation for the same time history.

As predicted by the approximate spectral method, drifts under rare earthquake are the one response quantity where the conventional scheme performs the best. Due to the sub-linear damping exponent, the effective damping of the damper scheme decreases with increasing lateral forces; under rare earthquake the damping of the FVD scheme is not large enough to compensate for the lower stiffness compared to the conventional scheme.

非线性时程分析

前一章节描述的受力和位移估计值虽然有助于理解周期和阻尼比等简单参数如何影响结构的整体性能，但估计值是近似值，仅考虑了一个振型，没有直接包括非线性的影响。更全面的方法是使用非线性时程分析评估结构性能。

对于每级地震，非线性时程分析中将采用相同的7组正交的地震动时程记录分别作用于三个模型 (传统外伸臂、BRB外伸臂、FVD外伸臂) 。用CSI的Perform 3D软件构建三个模型，除外伸臂构件外，三个模型完全相同，阻尼器模型不包括腰桁架。模型除了考虑了外伸臂、核心墙、周边框架柱、周边框架梁和腰桁架的材料非线性，还考虑了P-Δ 非线性; 非线性构件反应以ASCE 41-06的参数为基础。假设每种工况下的固有阻尼都是2%。

非线性时程分析结果

表3总结了时程分析结果。考虑的四种结果包括x向的底部倾覆力矩、x向的最大层间位移、外伸臂构件的能量耗散、结构体系其余构件 (连梁、核心墙、框架梁和腰桁架) 的能量耗散。最后一项结果可以作为其他结构构件所造成的破坏衡量指标。

对于各个模型和各级地震，报告了7组时程分析结果的平均值。结果具有与上一章节的近似结果类似的趋势，与传统结构方案相比，BRB方案和FVD方案的周期较长，阻尼较大，内力较小，能量耗散也较大。这反过来减少了其他结构构件的能量耗散，意味着BRB方案和FVD方案的结构破坏较小。

对BRB方案和FVD方案进行比较可以清楚地看出，可以清楚的看到，由于BRB在多遇地震作用下保持弹性，在设防地震作用下仅产生较小的屈服，因此阻尼器方案的能量耗散要大得多，尤其是地震比较低的情况。图8的滞回曲线显示了两种构件的不同表现，以及示例时程下的能量耗散的大小。类似的，图9的曲线显示了同一时程下各种构件的相对能量耗散比例。

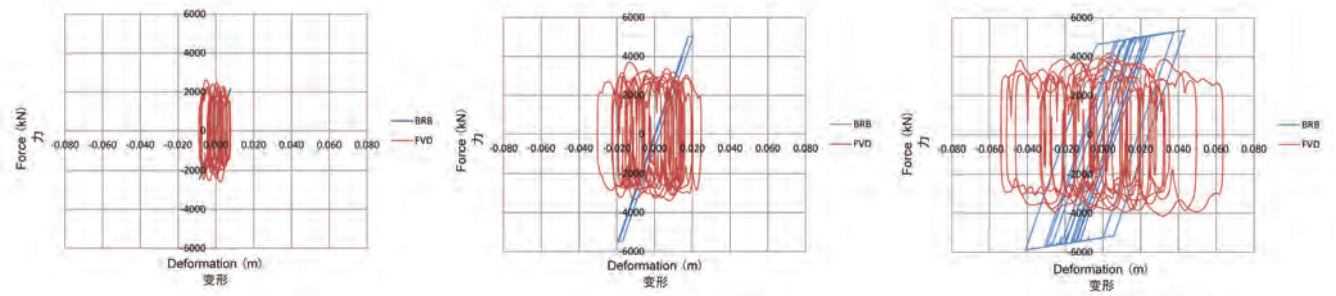

Figure 8. Hysteresis loops for selected BRB and FVD outrigger elements under sample frequent (left), moderate (center), and rare (right) earthquake time histories. (Source: Halvorson and Partners)
图8: 选定的BRB和FVD外伸臂构件在示例多遇 (左)，设防 (中) 和罕遇 (右) 地震作用时程分析的滞回曲线。(资料来源: 美国H+P建筑结构事务所)

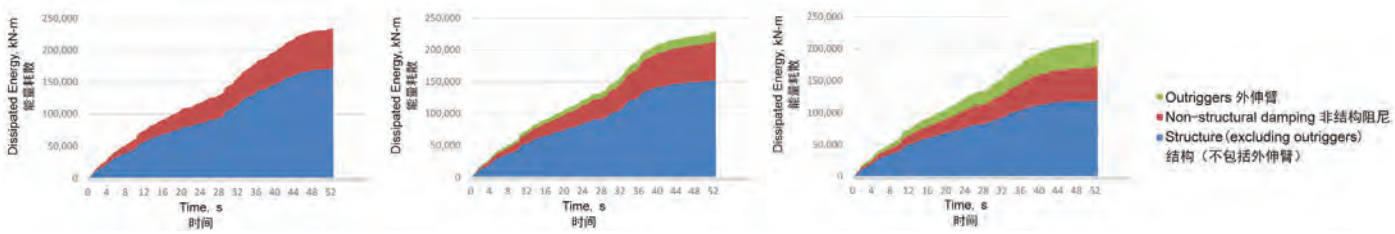

Figure 9. Energy dissipation vs. time under sample rare earthquake response history, conventional outrigger scheme (left), BRB scheme (center), and FVD scheme (right). (Source: Halvorson and Partners)
图9: 传统外伸臂方案 (左)、BRB方案 (中) 和FVD方案 (右) 在示例罕遇地震时程分析能量耗散vs时间 (资料来源: 美国H+P建筑结构事务所)

Conclusion

This study demonstrates that there are potentially significant advantages in replacing conventional steel outriggers with either BRB or FVD elements. The FVD scheme generally performed the best for the building considered, especially under service conditions (wind and frequent earthquake).

In addition to providing helpful energy dissipation and reducing global forces, both alternate schemes in this study meet performance objectives using outrigger elements with maximum forces significantly less than in the conventional scheme. This allows for significant reductions in the adjacent structure, including the core wall panel zone and associated connections. By avoiding outriggers which impose extremely large concentrated forces at small localized areas of the building, the result is a 'gentler' and arguably more natural structural system.

In situations where a high-rise structural design is controlled by drift under rare earthquake, or core wall stresses near the base of the building, a conventional outrigger scheme still has some advantages. But there are many other circumstances in which BRB or FVD outriggers may demonstrate superior structural performance, leading to a more economical solution. FVD outriggers appear particularly promising and merit serious consideration for both wind-controlled and seismic-controlled high-rise structures.

正如近似反应谱方法预测的那样，对于罕遇地震位移，传统方案表现最佳。由于次线性阻尼指数的关系，阻尼器方案的有效阻尼随着侧向力的增加而减少; 在罕遇地震条件下，FVD方案的阻尼不够大，不足以补偿小于传统方案的刚度。

结论

本项研究表明，用BRB构件或FVD构件代替传统外伸臂钢支撑有可能获得明显的优势。就本研究建筑物而言，FVD方案的总体性能最好，在正常使用状态 (风荷载和多遇地震作用) 下的性能尤其突出。

除了有助于能量耗散、减少整体受力以外，两种替代方案还满足外伸臂构件的性能目标，且最大受力明显小于传统方案。从而允许大幅减少相邻结构，包括核心墙节点域和相关连接。由于未使用在建筑物局部小范围区域大量集中应力的外伸臂，因此能形成更'温和'、更自然的结构体系。

在高层结构设计受罕遇地震位移或者建筑物底部核心墙应力控制的情况下，传统外伸臂方案仍然具有一定的优势。但在很多情况下，BRB外伸臂或FVD外伸臂具有优越的结构性能，能带来更经济的结构方案。FVD外伸臂的潜力巨大，在风荷载和地震作用控制的高层结构设计中值得认真考虑。

References (参考书目):

ASCE. (2006). ASCE 41-06 **Seismic Rehabilitation of Existing Buildings. Reston**, VA: American Society of Civil Engineers (ASCE).

ASCE. (2010). ASCE 7-10 **Minimum Design Loads for Buildings and Other Structures**. Reston, VA: American Society of Civil Engineers (ASCE).

Klemencic, R., Hooper, J., and Johansson, O. (2008). "One Rincon Hill: Raising the Bar." **Proceedings of the Structures Congress 2008**: pp. 1-11.

McNamara, R., Huang, C., and Wan, V. (2000). "Viscous-Damper with Motion Amplification Device for High-Rise Building Applications." **Proceedings of the Structures Congress 2000**, Advanced Technology in Structural Engineering: pp. 1-10.

Smith, R., and Willford, M. (2007). "The Damped Outrigger Concept for Tall Buildings." **The Structural Design of Tall and Special Buildings**. Volume 16, pp. 501-517. John Wiley & Sons, Ltd.

Taylor, D. (2003). "Mega Brace Seismic Dampers for the Torre Mayor Project at Mexico City." **Proceedings of the Shock and Vibration Symposium**, San Diego.